AIP Physics of Plasmas

Self consistent radio-frequency wave propagation and peripheral direct current plasma biasing: Simplified three dimensional non-linear treatment in the "wide sheath" asymptotic regime

L. Colas, J. Jacquot, S. Heuraux, E. Faudot, K. Crombé et al.

Citation: Phys. Plasmas **19**, 092505 (2012); doi: 10.1063/1.4750046

View online: http://dx.doi.org/10.1063/1.4750046

View Table of Contents: http://pop.aip.org/resource/1/PHPAEN/v19/i9

Published by the American Institute of Physics.

Self consistent radio-frequency wave propagation and peripheral direct current plasma biasing: Simplified three dimensional non-linear treatment in the "wide sheath" asymptotic regime

L. Colas,[1,a)] J. Jacquot,[1] S. Heuraux,[2] E. Faudot,[2] K. Crombé,[3] V. Kyrytsya,[4] J. Hillairet,[1] and M. Goniche[1]
[1]*CEA, IRFM, F-13108 Saint-Paul-lez-Durance, France*
[2]*IJL-P2M UMR 7198 CNRS, F-54506 Vandoeuvre les Nancy, France*
[3]*Department of Applied Physics, Ghent University, B-9000 Ghent, Belgium*
[4]*LPP-ERM/KMS, Association Euratom-"Belgian State," TEC Partner, Brussels, Belgium*

(Received 29 May 2012; accepted 7 August 2012; published online 12 September 2012)

A minimal two-field fluid approach is followed to describe the radio-frequency (RF) wave propagation in the bounded scrape-off layer plasma of magnetic fusion devices self-consistently with direct current (DC) biasing of this plasma. The RF and DC parts are coupled by non-linear RF and DC sheath boundary conditions at both ends of open magnetic field lines. The physical model is studied within a simplified framework featuring slow wave (SW) only and lateral walls normal to the straight confinement magnetic field. The possibility is however kept to excite the system by any realistic 2D RF field map imposed at the outer boundary of the simulation domain. The self-consistent RF + DC system is solved explicitly in the asymptotic limit when the width of the sheaths gets very large, for several configurations of the RF excitation and of the target plasma. In the case of 3D parallelepipedic geometry, semi-analytical results are proposed in terms of asymptotic waveguide eigenmodes that can easily be implemented numerically. The validity of the asymptotic treatment is discussed and is illustrated by numerical tests against a quantitative criterion expressed from the simulation parameters. Iterative improvement of the solution from the asymptotic result is also outlined. Throughout the resolution, key physical properties of the solution are presented. The radial penetration of the RF sheath voltages along lateral walls at both ends of the open magnetic field lines can be far deeper than the skin depth characteristic of the SW evanescence. This is interpreted in terms of sheath-plasma wave excitation. Therefore, the proper choice of the inner boundary location is discussed as well as the appropriate boundary conditions to apply there. The asymptotic scaling of various quantities with the amplitude of the input RF excitation is established. © *2012 American Institute of Physics*.
[http://dx.doi.org/10.1063/1.4750046]

I. INTRODUCTION

The emission of radio-frequency (RF) waves by complex antennae and their damping in the core of magnetized plasmas have been described for a long time by sophisticated first principle models in realistic geometry. Comparatively, the simulation of anomalous RF power losses in the plasma edge is still less advanced, although the non-linear wave-plasma interactions in the plasma edge often set the operational limits of RF heating systems. Peripheral ion cyclotron range of frequencies (ICRF, 30–100 MHz in present fusion devices) wave damping is attributed to a DC biasing of the edge plasma by RF-sheath rectification.[1] This non-linear process is usually modelled in analogy with a double Langmuir probe driven by an oscillating RF voltage, estimated as the field-line-integrated RF field $E_{//}$ parallel to the confinement magnetic field $\mathbf{B_0}$.[2] In this exercise, each open flux tube in the scrape-off layer (SOL) is considered as independent of its neighbours and $E_{//}$ is generally computed from conventional antenna codes in the absence of sheaths,[3,4] i.e., perfect electric conductors are assumed in direct contact with the plasma. This procedure, although clearly not self-consistent, was widely implemented as the only tool able to model realistic wave-launching structures.[5–15] It was shown to reproduce qualitatively some RF-induced SOL modifications observed around powered antennae.[6,8,10,11,16] Yet its quantitative validity is questionable.[17] Moreover, contradictions appeared with recent measurements, e.g., the scaling of rectified DC plasma potential with RF power,[18] the radial penetration of the plasma bias,[19] or the non-linear generation of edge DC currents by RF waves.[10,20,21] Although no consensus presently exists over an alternative approach, RF-sheath physics needs improvement towards the first principles.

In this prospect, Sec. II of this paper proposes to describe the RF wave propagation in the bounded SOL plasma self-consistently with the DC biasing of the SOL from both ends of open magnetic field lines. A minimal fluid approach is followed, inspired by earlier work on RF plasma discharges[22–24] and recently applied to tokamaks.[17,25,26] The RF and DC parts of the model are coupled by non-linear RF and DC sheath boundary conditions at both ends of open magnetic field lines. The approach, called SSWICH (self-consistent sheaths and waves for ion cyclotron heating[27]) allows interaction between neighbouring flux tubes *via* the exchange of

a)Author to whom correspondence should be addressed. Electronic mail: laurent.colas@cea.fr.

self-consistent RF and DC currents. This paper describes only a simplified framework, featuring slow wave only and lateral walls normal to $\mathbf{B_0}$. The possibility is kept however to excite the system by any 2D RF field map imposed at the outer boundary of the simulation domain, in order to simulate complex antenna structures.

Despite these simplifications, the problem in all its generality is of a great complexity. Its self-consistent resolution with realistic excitation can only be envisaged numerically. The convergence of the iterative resolution algorithm is not guaranteed. In any case, it is all the faster as the starting point is closer to the final solution. Multiple roots were evidenced in some circumstances.[26] In order to gain insight into the physical behaviour of the full non-linear DC + RF model, and to provide a good "first guess" for its iterative resolution, the self-consistent system is solved explicitly in the asymptotic limit when the width of the sheaths gets very large. This simplified regime is reached as the RF power launched by the ICRF antenna tends to infinity. From a practical point of view, this is also a critical regime since experimentally the deleterious plasma-wall interaction related to the sheaths gets exacerbated at high RF power.[18,28–30] Sections III and IV detail the asymptotic resolution for several configurations of the excitation and of the target plasma. The way to refine iteratively the solution from its asymptotic value is also outlined. Throughout the resolution, key physical properties of the solution are outlined: the radial propagation of the oscillating sheath voltages at both ends of the open magnetic field lines in the SOL; the asymptotic scaling of various quantities with the amplitude of the input RF excitation (or equivalently with the launched RF power). The validity of the asymptotic treatment is also discussed: Sec. IV proposes a quantitative criterion as a function of the simulation parameters that is tested numerically in Sec. V.

II. OUTLINE OF SSWICH MODEL

The proposed SSWICH model is thought as a minimal self-consistent RF + DC approach able to capture the experimental phenomenology outlined in the Introduction. It is motivated by a closer proximity to the first principles and the allowance for DC current circulation in the SOL. The model involves DC plasma quantities as well as harmonic RF waves oscillating at the ICRF wave frequency ω_0. RF and DC quantities are coupled non-linearly *via* two processes representing the sheath physics and implemented as boundary conditions. In many aspects, the RF model is inspired by Ref. 17. The problem is formulated in a fluid manner so that the concept of flux tube is less central than in the "standard approach."[5] The plasma medium is still highly anisotropic in the parallel direction. But the neighbouring field lines are coupled *via* RF and DC current exchanges and if they are sufficiently long, their two extremities can behave independently. Being minimal, the model is not fully complete in its present simplified formulation. No other frequency than 0 and ω_0 is considered and some transport coefficients remain phenomenological, contrary to Ref. 19. The RF model incorporates only one wave polarization (the slow wave) and the simulation geometry is restricted to parallelepipedic shape. Input plasma parameter profiles (density, temperatures) are prescribed, whereas RF-induced SOL profile modifications are highly suspected, e.g., density convection due to the differential biasing of neighbouring flux tubes.[6,16,29,31–33]

A. RF part of the model: Full-wave propagation in bounded 3-dimensional (3D) SOL plasma

The RF part of the model is sketched in Figure 1(a), where x, y, z denote, respectively, the local radial, poloidal, and parallel directions of a flattened tokamak. The simulation domain is a 3D collection of straight open field lines aligned along z in the SOL. For the sake of simplicity parallelepipedic geometry will be considered here, with parallel (respectively, radial) extension $L_{/\!/}$ ($L_\perp$). The physical concepts developed are, however, still valid in more complex 3D simulation domains whose boundaries are either parallel or normal to $\mathbf{B_0}$.[27] At the RF frequency ω_0, the SOL plasma is characterized by a gyrotropic dielectric tensor $\boldsymbol{\varepsilon}(x,\omega_0)$[34]

$$\boldsymbol{\varepsilon}(x,\omega_0) = \begin{bmatrix} \varepsilon_\perp & -i\varepsilon_\times & 0 \\ +i\varepsilon_\times & \varepsilon_\perp & 0 \\ 0 & 0 & \varepsilon_{/\!/} \end{bmatrix} \begin{matrix} x \\ y \\ z \end{matrix}. \tag{2.1}$$

Consistently with the cold plasma approximation, the SOL plasma is supposed to be spatially non-dispersive: the tensor $\boldsymbol{\varepsilon}(x,\omega_0)$ may depend on the radial coordinate x and on the frequency ω_0 but not on wave vectors, so that the wave equations can be easily expressed in configuration space rather than Fourier space. The gyrotropic medium is bi-refringent: in describing the RF field propagation, two polarizations need to be distinguished, the fast wave (FW) and the slow wave (SW). This paper focuses on the behaviour of the RF field $E_{/\!/}(x,y,z,\omega_0)$ parallel to the confinement magnetic field $\mathbf{B_0}$. In the limit when $|\varepsilon_{/\!/}|$ is high compared to other dielectric

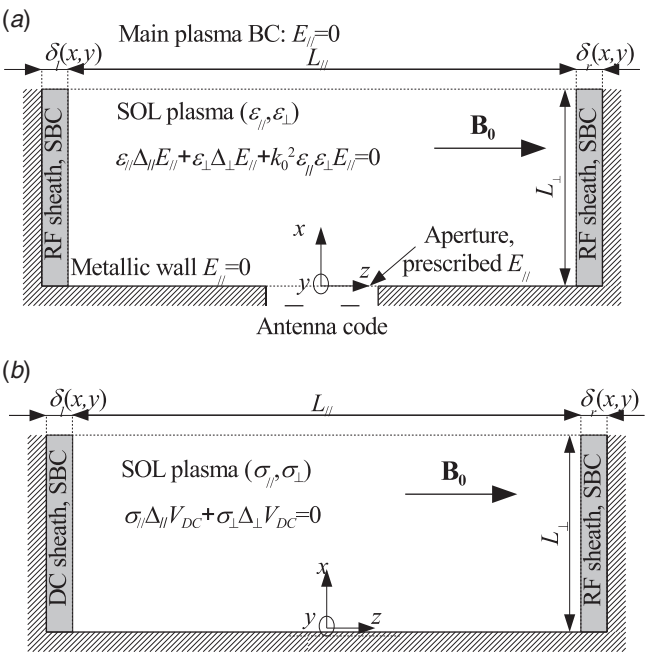

FIG. 1. Radial/toroidal cut through the 3D simulation domain. Outline of (a) the RF model and (b) the DC model.

constants and squared refractive indexes, $E_{//}(x,y,z,\omega_0)$ is entirely due to the SW and is governed by the wave equation

$$\varepsilon_{//}\Delta_{//}E_{//} + \varepsilon_{\perp}\Delta_{\perp}E_{//} + \varepsilon_{//}\varepsilon_{\perp}k_0^2E_{//} = 0. \quad (2.2)$$

In this expression, $k_0 = \omega_0/c$ is the wavevector in vacuum, Δ is the Laplace operator, the subscripts // and $\perp$ refer to the local directions parallel and transverse to $\mathbf{B_0}$. The high-$|\varepsilon_{//}|$ ordering used to derive (2.2) is generally valid in tokamak plasmas for the SW directly excited by RF antennae but will need discussion in our particular context for RF fields resulting from the interaction of the incident SW with the sheaths.

The RF waves are emitted through an aperture in the outer metallic chamber wall at the radial boundary $x = 0$. The RF electric field $\mathbf{E}$ is prescribed at this boundary. This input 2D mapping $E_{//ap}(y,z)$ is typically produced by an antenna code in the absence of sheaths and excites the whole RF + DC physical system. As suggested by Figure 1(a), the physical aperture might not extend over the whole parallel extension $L_{//}$ of the simulation domain. For the ease of notation, the whole radial plane $x = 0$ will be denoted "aperture," but the two cases whether $E_{//ap}$ is null or not at $z = \pm L_{//}/2$ will be distinguished since this affects the sheath excitation.

At the ICRF frequencies, the typical parallel dielectric constants $\varepsilon_{//}$ are highly negative even in the tenuous SOL plasma. Therefore, plane SW are evanescent for all parallel wave-numbers $k_{//}$ above a critical density corresponding to $\varepsilon_{\perp} = 0$. We suppose that this critical density is reached at the "main plasma" side of the simulation domain, i.e., $\varepsilon_{\perp} < 0$ at $x = L_{\perp}$. Therefore, the SW is assumed totally extinguished and metallic boundary conditions are enforced $E_{//}(x = L_{\perp}, y, z) = 0$. These inner boundary conditions, as well as the optimal choice of the radial depth $L_{\perp}$, will be further discussed in relation with the RF sheath radial penetration.

B. RF Sheath boundary conditions as a propagation equation for an oscillating sheath voltage

In the immediate vicinity of the ICRF launcher in the SOL, the so-called "open" magnetic field lines are bounded by lateral metallic parts, located in $z = \pm L_{//}/2$ in the parallelepipedic case. Between the bulk plasma and the metallic wall, a thin transition layer or sheath is established. Since the sheath usually has a width δ much thinner than the toroidal extension $L_{//}$ of the simulation domain, its consequence on the RF field propagation is accounted for *via* a RF "sheath boundary condition" (SBC) that replaces the usual metallic boundary condition. Although they rigorously prevail at the sheath/plasma interface, the RF-SBCs are applied directly at the wall. Presently, no SBC is applied at the metallic chamber wall containing the aperture in $x = 0$.

A simple RF-SBC for the RF electric field at the sheath-plasma interface was proposed in Ref. 17. This concept of SBC has already been successfully applied in the context of inductive[24] and capacitive[35] plasma discharges with unmagnetized plasma however. Implementing SBCs in the TOPICA antenna code was also attempted,[25] but in vacuum. Numerical implementation with magnetized plasma was only achieved recently in still very simple geometry.[26] At the RF frequency, the RF current through the sheath is supposed to be mainly a *displacement* current. In this framework, the sheath is assimilated to a parallel plate capacitor of width δ, filled with a dielectric material of dielectric constant ε_{sh}. This description is motivated since the sheath is a region depleted of electrons similar to vacuum. Inline with this view, the width δ is of the order of the (local, time averaged) sheath width. The dielectric constant is of the order of $\varepsilon_{sh} \sim +1$, while $\varepsilon_{//}$ in the SOL is highly negative. However in presence of high power waves, the "real" sheath width is subject to large amplitude RF oscillations around its mean value, which may affect the effective sheath capacitance.[22,23] Within these simple assumptions, the RF-SBC is linear and reads[17]

$$\mathbf{E_t^{(pl)}} = \nabla_{\mathbf{t}}\left(\delta D_n^{(pl)}/\varepsilon_{sh}\right) = \nabla_{\mathbf{t}}V_{rf}. \quad (2.3)$$

Here, $\mathbf{E}$ is the RF electric field, $\mathbf{D} = \boldsymbol{\varepsilon}\mathbf{E}$ is the RF electric displacement. RF quantities are evaluated at the plasma side of the sheath/plasma interface (superscript (pl)), where $\mathbf{D}$ is continuous and $\mathbf{E}$ exhibits a jump because the dielectric tensor $\boldsymbol{\varepsilon}$ changes abruptly. The subscripts n and t refer, respectively, to the direction locally normal (towards plasma) and transverse to the wall. The sheath width δ is allowed to vary spatially and its radial/poloidal distribution needs be subsequently determined self-consistently from the DC sheath potential. When the sheath width is null ($\delta = 0$), the RF-SBC (2.3) amounts to the usual metallic boundary conditions $\mathbf{E_t^{(pl)}} = \mathbf{0}$. The quantity $V_{rf} = \delta D_{\mathrm{n}}^{(\mathrm{pl})}/\varepsilon_{sh}$ at the right hand side (RHS) of Eq. (2.3) physically defines an oscillating RF voltage across the sheaths that drives the rectification of the DC plasma potential. V_{rf} is null in the absence of sheaths. When the wall is arbitrarily oriented with respect to $\mathbf{B_0}$, it was proved that Eq. (2.3) couples the FW and the SW at the lateral boundaries of the simulation domain, so that both modes need to be treated simultaneously to describe the RF sheath excitation.[36] Our restrictive geometry with lateral boundaries normal to $\mathbf{B_0}$ is essentially motivated by a simplified treatment to avoid the FW. Dropping the superscript (pl), the RF-SBC (2.3) becomes

$$\mathbf{E}_{\perp}(x,y,z = \pm L_{//}/2) = \mp\nabla_{\perp}(\delta\varepsilon_{//}E_{//}/\varepsilon_{sh}) = \mp\nabla_{\perp}V_{rf}. \quad (2.4)$$

The opposite signs for the opposite walls account for the reversal of the normal direction $\mathbf{n}$. Within the high-$|\varepsilon_{//}|$ ordering already introduced, $E_{//} = 0$ can be assumed for the cold FW. Thus, for this wave polarization, the simplified RF-SBC (2.4) amounts to the metallic boundary condition $E_{\perp} = 0$ and the FW does not excite RF sheaths in the present model. In Ref. 37, the same evaluation was performed using the full field polarization, including $1/|\varepsilon_{//}|$ contributions to $E_{//}$ from the FW. It was concluded that for plasma conditions and wave amplitudes typical in the vicinity of ICRF launchers, only modest sheath rectification was expected with walls normal to $\mathbf{B_0}$. This evaluation would deserve to be repeated in more realistic geometry. But within the present paper, only the SW is supposed to contribute to V_{rf} and will be kept below. Conservation of the RF electric displacement in the SOL plasma is expressed as

$$\mathrm{div}(\boldsymbol{\varepsilon}\mathbf{E}) \approx \varepsilon_\perp \mathrm{div}_\perp \mathbf{E}_\perp - i\varepsilon_\times (\mathbf{rot}\mathbf{E}_\perp)_{/\!/} + \varepsilon_{/\!/}\partial_{/\!/}E_{/\!/} = 0. \quad (2.5)$$

The SW RF field exhibits essentially a transverse magnetic polarization, so that $(\mathbf{rot}\mathbf{E}_\perp)_{/\!/} \ll \mathrm{div}_\perp \mathbf{E}_\perp$. Using the simplified SBC (2.4) allows eliminating $\mathbf{E}_\perp$, yielding a new boundary condition for the SW involving $E_{/\!/}$ only[38]

$$\begin{aligned}\varepsilon_\perp \Delta_\perp V_{rf} &= \varepsilon_\perp \Delta_\perp (\varepsilon_{/\!/}\delta E_{/\!/}/\varepsilon_{sh}) \\ &= \pm\varepsilon_{/\!/}\partial_{/\!/}E_{/\!/}(x,y,z=\pm L_{/\!/}/2). \end{aligned} \quad (2.6)$$

In addition to the SW, the RF SBCs (2.6) allow the propagation of an additional wave branch in the SOL plasma. This sheath-plasma wave (SPW), whose RF electric field is mainly concentrated near the lateral walls, exists only in presence of the sheaths and features dispersion properties quite different from the SW.[17] The SPW is essential in the development of the RF sheaths and will be detailed below. This new degree of freedom makes it convenient to treat the RF voltage V_{rf} as a new unknown independent of $E_{/\!/}$. In this prospect, the left hand side of Eq. (2.6) can be regarded as a transverse propagator for V_{rf} with a source term at the RHS. This philosophy will guide our asymptotic resolution.

C. DC biasing of the plasma via RF sheath rectification

1. General model

The DC part of the SSWICH problem is sketched in Figure 1(b). It is treated in the same way as the RF fields, i.e., via a partial differential equation for the electrostatic DC plasma potential $V_{DC}(x,y,z)$ expressing the local balance of electric charge over the same 3D simulation volume as for the RF problem.

$$\sigma_{/\!/DC}\Delta_{/\!/}V_{DC} + \sigma_{\perp DC}\Delta_\perp V_{DC} = 0. \quad (2.7)$$

In this expression, the constants $(\sigma_{/\!/\mathrm{DC}}, \sigma_{\perp\mathrm{DC}})$ describe the DC plasma conductivity parallel and transverse to $\mathbf{B_0}$. $\sigma_{/\!/\mathrm{DC}}$ is the Spitzer DC parallel conductivity. Rigorously, the transverse DC plasma conductivity takes the form of a diffusion operator $\sigma_{\perp\mathrm{DC}}\Delta_\perp V_{DC}$ only in the case of ion-neutral collisions.[39] However, the effective transverse DC conductivity of tokamak SOL plasmas is far more intense than expected from ion-neutral collisions alone. Finding its physical nature is in itself a topic of active research. Many physical processes were outlined in the literature to account for the observations: ion viscosity, inertia, or anomalous transport.[39,40] It is outside the scope of the present model to reproduce the detailed conduction mechanism: here it is represented phenomenologically as an effective perpendicular conductivity $\sigma_{\perp\mathrm{DC}}$.

The formalism outlined in (2.7) allows DC currents to flow in the bulk plasma. Through this process, a given sheath gets coupled to its neighbours as well as with the sheath at the opposite wall along the same field line. This non-locality was investigated in Refs. 41 and 42 and needs to be accounted for in order to reproduce the measured DC currents created by RF sheaths during ion cyclotron resonance heating (ICRH).[10,21] The DC part of model[17] is recovered in the limit $(\sigma_{/\!/\mathrm{DC}}, \sigma_{\perp\mathrm{DC}}) = (0,0)$.

To fully specify the DC problem, Eq. (2.7) should be complemented with appropriate DC sheath boundary conditions for V_{DC} at plasma/sheath interfaces. For the RF problem, the sheaths were assimilated to parallel-plate capacitors, i.e., it was implicitly assumed that the RF current through the sheaths was predominantly a (linear) *displacement* current. When dealing with DC currents, the *conduction* currents through the sheaths need to be explicitly accounted for. Since the sheath exhibits a non-linear I-V characteristic, a rectification process occurs that couples the RF and DC parts of our physical model. At both ends of the open flux tubes, the instantaneous voltage across the sheaths is supposed to be composed of a DC part and of a RF part oscillating at the RF frequency ω_0. No other frequency is considered, contrary to Ref. 19. At the left sheath

$$V_l(x,y,z=-L_{/\!/}/2,t) = V_{DCl}(x,y) + V_{rfl}(x,y)\cos(\omega_0 t + \varphi). \quad (2.8)$$

The RF part of the voltage is provided by the solution of the RF problem: it is the quantity V_{rf} already introduced in Eq. (2.3). The walls are assumed electrically grounded, so that the DC sheath potential $V_{DCl}(x,y)$ is also the local DC plasma potential used in Eq. (2.7). Associated to the instantaneous sheath voltage, the instantaneous *conduction* current into the sheath reads

$$I_l(x,y,z=-L_{/\!/}/2,t) = i^+(1-\exp(e(V_f - V_l(t))/kT_e)). \quad (2.9)$$

In this expression, i^+ is the local ion saturation current, T_e is the local electron temperature, and V_f is a local floating potential in the absence of RF waves. This I-V electrical characteristic was rigorously established for DC sheaths with normal $\mathbf{B_0}$. It is presently extended to a dynamical regime. More elaborate treatments of the conduction current in RF sheaths were proposed in the context of un-magnetized RF plasma reactors.[22,23] No equivalent presently exists with tilted $\mathbf{B_0}$, like the Chodura model for DC sheaths.[43] The DC part of I_l is obtained by time averaging Eq. (2.9)

$$\begin{aligned}&\langle I_l(x,y,z=-L_{/\!/}/2)\rangle/i^+ \\ &\quad = 1 - \exp\big(e(V_f - V_{DCl})/kT_e\big)\mathrm{I}_0(e|V_{rfl}|/kT_e). \end{aligned} \quad (2.10)$$

In this expression, $\langle\ldots\rangle$ means time-average over one RF period and $\mathrm{I}_0(\ldots)$ is the modified Bessel function of order 0. The general DC SBCs state that the local DC current leaving the bulk plasma is the DC current into the sheath: using expression (2.10), this requirement yields a non-linear DC SBC

$$\begin{aligned}&i^+\big[1 - \exp\big(e\big(V_f + V_{bl} - V_{DC}\big)/kT_e\big)\big] \\ &\quad = [\sigma_{\mathbf{DC}}.\nabla V_{DC}]_\mathrm{n} = \sigma_{/\!/\mathrm{DC}}\partial_{/\!/}V_{DC}(x,y,z=-L_{/\!/}/2). \end{aligned} \quad (2.11)$$

In this expression, we have defined the potential

$$V_{bl}(x,y) = kT_e \ln\big[\big(\mathrm{I}_0\big(e|V_{rfl}|(x,y)/kT_e\big)\big]/e \geq 0. \quad (2.12)$$

V_{bl} plays the role of a localized, positive DC bias. Although the vacuum vessel is electrically grounded, the sheath rectification of V_{rfl} acts in practice as if the DC bias V_{bl} was applied at vessel wall. Contrary to conventional biasing experiments, V_{bl} can be spatially inhomogeneous over the lateral walls. In the absence of volume source term in Eq. (2.7), this RF → DC coupling uses RF fields $E_{//}$ to drive the DC biasing from field line extremities.

2. Simplified more local DC biasing model

Due to Eq. (2.7) allowing global DC current exchanges, the general DC problem is non-local: RF excitation of one sheath enhances the DC plasma potential in its entire neighbourhood as well as at the opposite side of the open flux tube. Besides, its DC-SBCs (2.11) make the DC problem non-linear. Therefore, it can only be solved numerically. In order to yield analytically tractable solutions, it is simplified here in the limit of infinite parallel conductivity and negligible transverse conductivity. Assuming perfect plasma DC parallel conductivity $\sigma_{//\mathrm{DC}}$ suppresses any DC potential drop along a field line in the bulk plasma. The DC plasma potential $V_{DC}(x,y)$ is then determined by requiring that the sum of the parallel DC currents into the two opposite sheaths balances the transverse DC current across the field line. In the limit of negligible transverse conductivity $\sigma_{\perp\mathrm{DC}}$, this transverse DC current is taken null. The final DC current balance reads

$$i^{+}\left[2-\exp\left(e(V_f-V_{DC}+V_{bl})/kT_e\right)-\exp\left(e(V_f-V_{DC}+V_{br})/kT_e\right)\right]=0. \tag{2.13}$$

Relation (2.13) is more local in that every flux tube behaves independently of its neighbours. Yet the parallel conductivity couples the sheaths at both extremities of a field line. Relation (2.13) defines the DC plasma potential $V_{DC}(x,y)$ on flux tube (x,y) as a function of the RF excitations at its two ends. Namely, $V_{DC}(x,y)=V_f+V_b(x,y)$ with a composite bias $V_b(x,y)$

$$\begin{aligned} eV_b(x,y) &\equiv e(V_{bl}+V_{br})/2+kT_e\ln[\cosh[e(V_{bl}-V_{br})/2kT_e]] \\ &= kT_e\ln\left[\left((\mathrm{I}_0(e|V_{rfl}|/kT_e)+\mathrm{I}_0(e|V_{rfr}|/kT_e)\right)/2\right]. \end{aligned} \tag{2.14}$$

D. Second RF-DC coupling: Self-consistent sheath capacitance

The above models described how the RF part of the fields influences the DC potentials *via* sheath rectification. In turn, the DC potentials act non-linearly on the RF fields through the self-consistent sheath capacitance that needs to be introduced into the SBC (2.3) for the RF problem. To keep the problem simple, it is assumed that despite its high amplitude RF oscillation, the (time-averaged, local) sheath width δ follows the Child-Langmuir law for plane electrodes:[44,45]

$$\delta(x,y)=\lambda_e(eV_{DC}/kT_e)^{3/4}. \tag{2.15}$$

In this expression, λ_e is the electron Debye length. $\delta(x,y)$ is *a priori* inhomogeneous transverse to $\mathbf{B_0}$, since the RF fields (and hence the DC potentials $V_{DC}(x,y)$) are expected to evolve radially. The Child-Langmuir law was established for collision-less DC sheaths. More sophisticated models developed in the context of capacitive RF plasma devices indicate that the actual RF sheath width is $(50/27)^{1/2}\sim 1.36$ times larger than predicted by Eq. (2.15), while the effective dielectric constant in the sheath capacitance is $\varepsilon_{sh}\sim 1.226$.[22] So the ratio δ/ε_{sh} is approximately correct in the expression of V_{rf}. These results are valid for high amplitude collision-less RF sheaths parallel to $\mathbf{B_0}$ in planar geometry, with immobile ions and inertia-less electrons ($\omega_{pi}\ll\omega_0\ll\omega_{pe}$). This is enough to deal with tokamak RF sheaths in our simplified parallepipedic geometry. Other more elaborate formulae exist in the literature (e.g., Ref. 23) and could progressively replace the simpler ones. The counterpart is the generation of harmonic frequencies of ω_0. In the prospect of a generalization for our model, expression (2.15) would also require revision to account for shaped lateral walls (e.g., Ref. 46 for DC sheaths in cylindrical geometry) with oblique incidence of the magnetic field lines.

III. ASYMPTOTIC RESOLUTION FOR "WIDE SHEATHS:" LEADING ORDER SOLUTION FOR $E_{//}\neq 0$ AT LATERAL BOUNDARIES OF ANTENNA APERTURE

A. Motivations and principle of the new method

Despite the simplifications envisaged in this paper, the SSWICH problem is fairly complex. To compute the SW fields $E_{//}$ in presence of RF-SBCs, it is necessary to know the 2D (radial/poloidal) spatial distribution $\delta(x,y)$ of the sheath widths along lateral boundaries of the simulation domain, *via* the RF voltages V_{rf} in Eq. (2.4). $\delta(x,y)$ comes from the DC biasing problem *via* the Child-Langmuir law (2.15), and in turn knowing the 2D map $E_{//}(x,y)$ at the lateral boundaries is necessary to solve the sheath rectification. Therefore, a "first guess" into the self-consistent loop is valuable.

In order to solve for the RF field, a widespread technique consists in separating it into a set of toroidal eigenmodes.[17,36–38] In presence of RF-SBCs, these eigenmodes are only well defined if parameter $\Lambda\equiv-\delta\varepsilon_{//}/(L_{//}\varepsilon_{sh})$ can be treated as a constant.[17] However in realistic situations, the dielectric tensor has a radial profile, the self-consistent sheaths can adopt different widths at the two lateral boundaries, and the 2D map $\delta(x,y)$ is generally inhomogeneous over similar spatial scale-lengths as the RF field. Reference 17 explored the issue of spatially varying sheath widths, when the concept of eigenmode gets blurred. But this study was restricted to one "mode" in a weakly inhomogeneous limit ("small" radial gradient of Λ, no mode coupling, etc.). Besides, eigenmodes can hardly be generalized to more complex geometries than parallelepipedic (e.g., Ref. 27). These difficulties motivated an alternative method to find a first guess for the self-consistent solution of the RF + DC problem in realistic situations without relying on RF field eigenmodes. The general method is valid whatever the 2D input RF field map, in presence of a radial profile for the plasma parameters, and with no assumption *a priori* about the self-consistent 2D sheath widths distribution $\delta(x,y)$ that

emerges as an output. The counterpart is a restricted validity domain.

For the purpose of RF sheath assessment in tokamak environment, a critical situation arises when the DC biasing gets very intense. From Child-Langmuir law (2.15), the sheath widths δ then grow very large. In this "wide sheath regime," it was early noticed that the RF SBCs (2.4) or (2.6) get simplified, some physical quantities becoming nearly independent of δ.[17,38] The principle is then to split the fields in the problem (e.g., V_{rf}) into successive approximations

$$V_{\mathrm{rf}}(x,y,z) = V_{rf}{}^{(0)}(x,y,z) + V_{rf}{}^{(1)}(x,y,z) + \ldots. \quad (3.1)$$

With at the lateral boundaries

$$V_{rf}^{(1)}(x,y,z=\pm L_{/\!/}/2) = \frac{\lambda_{crit}}{\delta(x,y)} V_{rf\,cor}(x,y,z=\pm L_{/\!/}/2). \quad (3.2)$$

In this formula, λ_{crit} is a characteristic length that will be determined below from the parameters of the model. Under this form, the problem formally exhibits a non-dimensional parameter $\lambda_{crit}/\delta(x,y)$ that will be assumed small in the "wide sheath regime." The asymptotic treatment mainly consists in solving RF-SBCs (2.3) or (2.6) in perturbations with respect to this small parameter. Since from the RF viewpoint the sheath is assimilated to a capacitance, the asymptotic approach is also valid if the lateral walls are covered with a thick layer of dielectric material,[47] as was experimented in several tokamaks.[18,48] However in presence of a dielectric wall, the DC SBCs (2.11) need to be revised so that no DC current crosses the sheaths. Formally, the small parameter $\lambda_{crit}/\delta(x,y)$ depends on space so that sheaths need in principle to be wide *everywhere* for the expansion to converge. The validity of the approximations made will be discussed more deeply below.

Section III describes a self-consistent non-linear resolution of the RF + DC SSWICH problem at the leading order in the asymptotic expansion when the 2D RF field $E_{/\!/\mathrm{ap}}(y,z)$ applied at the aperture exhibits a non-zero value at the lateral sides of the simulation domain $z = \pm L_{/\!/}/2$. Section IV will perform the same exercise at the next order when the $E_{/\!/\mathrm{ap}}(y,z)$ is null at both lateral sides.

B. Radial penetration of RF voltages along lateral walls

At the leading order in the small parameter $\lambda_{crit}/\delta(x,y)$, the RF-SBCs (2.6) read at both sides of the simulation domain

$$\Delta_\perp\left(\varepsilon_{/\!/}\delta E_{/\!/}^{(0)}/\varepsilon_{sh}\right) = \Delta_\perp V_{rf}^{(0)} = 0. \quad (3.3)$$

At the inner radial boundary $x = L_\perp$, the metallic boundary conditions impose

$$V_{rf}{}^{(0)}(x = L_\perp, y, z = \pm L_{/\!/}/2) = 0. \quad (3.4)$$

The two above equations are still valid in the presence of a radially inhomogeneous dielectric tensor. They allow solving for $V_{rf}{}^{(0)}(x,y,z=\pm L_{/\!/}/2)$ along the lateral boundaries from the RF voltages at the aperture, without knowing *a priori* the self-consistent 2D spatial distribution of $\delta(x,y)$. We proceed by splitting $V_{rf}{}^{(0)}$ into a set of harmonic components oscillating as $\exp(ik_y y)$ in the direction y, assumed periodic in a flattened tokamak. The solution for the Fourier component $V_{rf}{}^{(0)}(x,k_y)$ takes the form

$$V_{rf}^{(0)}(x,k_y) = V_{rf}^{(0)}(0,k_y)\sinh\left(k_y(L_\perp - x)\right)/\sinh(k_y L_\perp). \quad (3.5)$$

The penetration depth of the RF voltages can be estimated as $\min(L_\perp, 1/|k_y|)$ and can, therefore, be far larger than the plasma skin depth $\lambda_{skin} \sim c/\omega_{pe}$ characteristic of the SW evanescence. The reason is that this penetration is *not* governed by the SW equation (2.2) but by the asymptotic RF SBC (3.3). From Ref. 17 in the asymptotic limit $\lambda_{crit}/\delta \to 0$, Eq. (3.3) describes the direct excitation of the SPW by the near RF voltage at the antenna aperture. Equation (3.3) shows that the asymptotic SPW equation applies with less restriction to $V_{rf}^{(0)}$ than to $E_{/\!/}$, for which homogeneous δ would be needed. The radial penetration of the RF voltages calls for further discussion of the metallic boundary conditions at the inner limit of the simulation volume, as well as of a proper physical choice of the radial depth $L_\perp$. Initially the inner plasma boundary was placed radially well beyond λ_{skin}, so that it plays no role with respect to the SW. If $k_y L_\perp \gg 1$, the radial location $L_\perp$ neither plays any role for the SPW and $L_\perp$ can be chosen with some latitude. If $k_y L_\perp \ll 1$, the SPW can propagate inward in the SOL plasma as long as lateral material boundaries are present. However, the SPW cannot propagate further in the free plasma in the absence of lateral walls. Given the very simple parallelepipedic geometry considered in this paper, a physically logical choice for $L_\perp$ is then the inner radial limit of the material objects surrounding the RF antenna (side limiters,[27] blanket shielding modules,[49]…). More clever choices can be envisaged in more complex geometries with material objects protruding inside a parallelepipedic domain (e.g., Ref. 27).

C. Self-consistent leading order RF + DC problem

The leading-order RF voltages at the antenna aperture need now to be determined self-consistently, taking into account the DC part of the SSWICH problem. Although the most general DC biasing model could be employed numerically, we proceed here with the simplified version in the limit $(\sigma_{/\!/\mathrm{DC}}, \sigma_{\perp\mathrm{DC}}) = (\infty, 0)$. $V_{rf}{}^{(0)}(x=0,y)$ is then determined from the coupled algebraic equations (2.14) and (2.15), using as input the RF field values $E_{/\!/l} = E_{/\!/\mathrm{ap}}(y, z = -L_{/\!/}/2)$ and $E_{/\!/r} = E_{/\!/\mathrm{ap}}(y, z = +L_{/\!/}/2)$ prescribed at the lateral sides of the aperture. We are mainly interested in the case $e|V_{rfl}|/kT_e \gg 1$, $e|V_{rfr}|/kT_e \gg 1$ when the DC plasma potential is highly enhanced compared to its value without RF waves. In this limit, the system can be solved explicitly and yields

$$\left|\frac{eV_{rfl}}{kT_e}\right| = \left[\frac{e\lambda_e}{kT_e}\frac{|\varepsilon_{/\!/}|}{\varepsilon_{sh}}\right]^4 E_{/\!/m}^3 |E_{/\!/l}|; \left|\frac{eV_{rfr}}{kT_e}\right| = \left[\frac{e\lambda_e}{kT_e}\frac{|\varepsilon_{/\!/}|}{\varepsilon_{sh}}\right]^4 E_{/\!/m}^3 |E_{/\!/r}|. \quad (3.6)$$

With $E_{/\!/m} \equiv \max(|E_{/\!/l}|, |E_{/\!/r}|)$,

$$\frac{eV_{DC}}{kT_e} = \left[\frac{e\lambda_e}{kT_e}\frac{|\varepsilon_{/\!/}|E_{/\!/m}}{\varepsilon_{sh}}\right]^4, \tag{3.7}$$

$$\frac{\delta}{\lambda_e} = \left[\frac{e\lambda_e}{kT_e}\frac{|\varepsilon_{/\!/}|E_{/\!/m}}{\varepsilon_{sh}}\right]^3. \tag{3.8}$$

The coordinates $(x=0,y)$ are implicit in the above formulae. From these results, both sides of the aperture get coupled in the self-consistent RF + DC problem. Besides, at the leading order of the asymptotic expansion, the self-consistent DC plasma potentials scale like the power four of the amplitude of the RF field at the sides of the aperture. Raising $E_{/\!/\mathrm{ap}}$ is equivalent to increasing the RF power P_{RF} launched by the ICRF antenna, with $E_{/\!/\mathrm{ap}} \propto {P_{RF}}^{1/2}$. Therefore, a parametric scaling as ${P_{RF}}^2$ is predicted for the leading order contribution to the sheath voltages.

RF voltages ${V_{rfl}}^{(0)}(x,y)$ and ${V_{rfr}}^{(0)}(x,y)$ have now been fully determined, making it possible to completely solve the DC problem and to deduce the self-consistent 2D distribution of sheath widths $\delta_l(x,y)$ and $\delta_r(x,y)$ at both extremities of every flux tube using Eq. (2.15). Finally, the leading order RF electric field ${E_{/\!/}}^{(0)}(x,y,z)$ is solved from the SW equation (2.2) complemented with the Dirichlet boundary conditions.

$$\begin{aligned}
&E_{/\!/}^{(0)}(x=0,y,z) = E_{/\!/ap}(y,z), \quad E_{/\!/}^{(0)}(x=L_\perp,y,z)=0,\\
&E_{/\!/}^{(0)}\left(x,y,z=-\frac{L_{/\!/}}{2}\right) = \frac{\varepsilon_{sh}V_{rfl}^{(0)}(x,y)}{\varepsilon_{/\!/}(x)\delta_l(x,y)},\\
&E_{/\!/}^{(0)}\left(x,y,z=+\frac{L_{/\!/}}{2}\right) = \frac{\varepsilon_{sh}V_{rfr}^{(0)}(x,y)}{\varepsilon_{/\!/}(x)\delta_r(x,y)}.
\end{aligned} \tag{3.9}$$

${E_{/\!/}}^{(0)}$ cannot generally be decomposed into eigenmodes, due to the lateral BCs with spatially inhomogeneous sheath widths. These BCs can be interpreted as if part of the RF field was excited from the *lateral sides* of the flux tubes and propagates in the *parallel* direction. Equation (3.9) also suggests that the self-consistent ${V_{rf}}^{(0)}$, δ, and lateral ${E_{/\!/}}^{(0)}$ are spatially inhomogeneous with similar scale-lengths. From the scaling considerations in Eqs. (3.6) and (3.8), ${E_{/\!/}}^{(0)}$ is proportional to the magnitude $E_{/\!/ap}$ of the RF excitation at the aperture. The fact that ${V_{rfl}}^{(0)}$ and ${V_{rfr}}^{(0)}$ grow faster than ${E_{/\!/}}^{(0)}$ with increasing $E_{/\!/ap}$ justifies *a-posteriori* dropping the right hand side term in Eq. (2.6) at the leading order. From the above discussion of RF voltage penetration, ${E_{/\!/}}^{(0)}$ at the lateral sides can exhibit rather large wavelengths in the radial direction. In these conditions, the SW equation (2.2) becomes questionable, as it was developed using the ordering $k_\perp \gg k_0|\varepsilon_\perp|$. The validity of Eq. (2.2) was discussed in Ref. 36, as well as possible alternative SW equations. It is outside the scope of the present paper to apply these alternative equations.

D. Iterative solution refinement

The RF + DC SSWICH problem was solved self-consistently at the leading order in the asymptotic expansion (3.1). This asymptotic approximation can then be used as the starting point of an iterative numerical refinement of the solution according to the following scheme:

(1) Solve for oscillating voltages at step n from the sheath BCs (2.6)

$$\Delta_\perp {V_{rfl}}^{(n)}(x,y) = \pm\frac{\varepsilon_{/\!/}(x)}{\varepsilon_\perp(x)}\partial_{/\!/}{E_{/\!/}}^{(n-1)}(x,y,z=\pm L_{/\!/}/2). \tag{3.10}$$

Consistently with the asymptotic ordering (3.1), the RHS of Eq. (3.10) at step n uses the lateral RF fields obtained at step n-1.

(2) Solve the DC problem at step n from the RF voltages at step n and update the sheath widths from Child Langmuir law.

(3) Deduce the RF field map ${E_{/\!/}}^{(n)}$ at step n from the SW equation in the simulation volume using the lateral boundary conditions (3.9) updated at step n.

This can be regarded as a 3-fluid formulation of the original RF + DC model, where the quantity V_{rf} is treated as independent of $E_{/\!/}$ and accounts for the new degrees of freedom (the SPWs) introduced by the RF-SBCs. The method can be implemented numerically on more complex simulation domains than parallelepipedic, as long as side boundaries are kept normal to $\mathbf{B_0}$ (e.g., Ref. 27). The convergence of this iterative procedure remains an open issue in the general case. However within the asymptotic framework, this amounts to a set of successive small corrections. Section IV applies this procedure at the first order.

IV. ASYMPTOTIC RESOLUTION FOR "WIDE SHEATHS:" FIRST ORDER SOLUTION WHEN $E_{/\!/}=0$ AT LATERAL BOUNDARIES OF ANTENNA APERTURE

In many situations of physical interest, the lateral walls are located toroidally far away from the extremities of the physical aperture (see Figure 1). In the case of recessed antennae, this physical aperture is surrounded by a perfect metallic wall, where $E_{/\!/ap}(y,z)=0$ is prescribed.[4] A similar situation would arise if the RF + DC system was excited by current straps in the simulation volume instead of a prescribed field map at the outer boundary: In this case, the entire outer wall would be metallic. Section III showed that when $E_{/\!/\mathrm{ap}}(x=0,y,z=\pm L_{/\!/}/2)=0$, no RF sheath voltage develops at the leading order in the asymptotic expansion of the self-consistent RF + DC model. In this situation, the first order is the lowest relevant one and is treated below.

A. RF sheath voltages at first order

From Sec. III, in the particular case when $E_{/\!/\mathrm{ap}}(y,z=\pm L_{/\!/}/2)=0$, the three spatial coordinates get separable in ${E_{/\!/}}^{(0)}(x,y,z)$ and the spectral component ${E_{/\!/}}^{(0)}(x,k_y,z)$ takes the form

$$E_{/\!/}^{(0)}(x,k_y,z) = \sum_{n=1}^{\infty} E_n(k_y)\sin\left(k_{/\!/n}(z+L_{/\!/}/2)\right)F_n(x,k_y), \tag{4.1}$$

with $k_{/\!/n} \equiv n\pi/L_{/\!/}$. The eigenmodes in Eq. (4.1) are the asymptotic limits of similar SW modes as in Ref. 38. In our context, however, harmonic poloidal variation was added,

the inner BCs were changed, and inhomogeneous plasma was allowed. As $\delta \to \infty$, the eigenmodes become independent of Λ and can be used without restriction. The spectral coefficients $E_n(k_y)$ are obtained by projection of the input RF field map onto the eigenmodes. In the general case, the radial structure function $F_n(x,k_y)$ is solution of the SW equation (2.2) with simple BCs.

$$\partial^2_{xx}F_n(x,k_y) = [\varepsilon_{/\!/}(x)k_0^2 - k_{/\!/n}^2\varepsilon_{/\!/}(x)/\varepsilon_\perp(x) - k_y^2]F_n(x,k_y),$$
$$F_n(0,k_y) = 1, \quad F_n(L_\perp,k_y) = 0. \tag{4.2}$$

For homogeneous plasmas, this simplifies into

$$F_n(x,k_y) = \sin h\Big(k_{xn}(L_\perp - x)\Big)/\sin h(k_{xn}L_\perp),$$
$$k_{xn}^2 - k_y^2 = k_{\perp n}^2 = -\varepsilon_{/\!/}(k_0^2 - k_{/\!/n}^2/\varepsilon_\perp). \tag{4.3}$$

The asymptotic SW eigenmodes do not however contribute to $V_{rf}^{(0)}$. $V_{rf}^{(1)}$ therefore needs to be determined from Eq. (2.6) expanded at the first order

$$\Delta_\perp V_{rf}^{(1)} = \pm\frac{\varepsilon_{/\!/}(x)}{\varepsilon_\perp(x)}\partial_{/\!/}E_{/\!/}^{(0)}(x,y,z=\pm L_{/\!/}/2),$$
$$V_{rf}^{(1)}(x=0,y,z) = V_{rf}^{(1)}(x=L_\perp,y,z) = 0. \tag{4.4}$$

The first order problem (4.4) is valid in presence of inhomogeneous plasma and can be evaluated explicitly without prior knowledge of the self-consistent 2D spatial distribution $\delta(x,y)$. The Fourier component $V_{rfl}^{(1)}(x,k_y)$ can be expressed as the convolution of the spectral RHS source term with a Green's function

$$V_{rfl}^{(1)}(x,k_y) = \int_0^{L_\perp}\frac{\varepsilon_{/\!/}(x')}{\varepsilon_\perp(x')}\frac{\partial_{/\!/}E_{/\!/}^{(0)}}{k_y}\left(x',k_y,z=-\frac{L_{/\!/}}{2}\right) \times G(k_yx,k_yx',k_yL_\perp)dx'. \tag{4.5}$$

The Green's function $G(X,X',X_1)$ is solution of the normalized problem (4.4) with a Dirac source term

$$G(X,X',X_1) = \frac{\sin h(X_{\min})\sin h(X_1 - X_{\max})}{\sin h(X_1)},$$
$$X_{\min} = \min(X,X'), \quad X_{\max} = \max(X,X'). \tag{4.6}$$

Since $V_{rf}^{(1)}$ depends linearly on $E_{/\!/}^{(0)}$, the RF voltage is the sum of contributions by each asymptotic SW mode *via* convolution (4.5). For homogeneous plasmas, Eq. (4.5) involves

$$\int_0^{L_\perp} G(k_yx,k_yx',k_yL_\perp)F_n(x',k_y)dx'$$
$$= \int_0^{L_\perp} G(k_yx,k_yx',k_yL_\perp)\frac{\sin h(k_{xn}(L_\perp - x'))}{\sin h(k_{xn}L_\perp)}dx' = \ldots$$
$$\ldots = \frac{k_y}{k_{\perp n}^2}\left[\frac{\sin h\big(k_y(L_\perp - x)\big)}{\sin h(k_yL_\perp)} - \frac{\sin h(k_{xn}(L_\perp - x))}{\sin h(k_{xn}L_\perp)}\right]. \tag{4.7}$$

Using the property $\left[\partial_{/\!/}\sin\big(k_{/\!/n}(z + L_{/\!/}/2)\big)\right]_{z=-L_{/\!/}/2} = k_{/\!/n}$, one deduces

$$V_{rfl}^{(1)}(x,k_y) = \sum_{n=1}^{\infty} V_{rfln}(x,k_y),$$
$$V_{rfln}(x,k_y) = \frac{k_{/\!/n}E_n(k_y)}{k_{/\!/n}^2 - k_0^2\varepsilon_\perp}S\left(k_xx,k_xL_\perp,\frac{k_y}{k_x}\right). \tag{4.8}$$

Similarly at the other side of the simulation domain $V_{rfrn}(x,k_y) = (-1)^{n+1}V_{rfln}(x,k_y)$. The radial dependence of V_{rf} for homogeneous plasmas is given by the shape function $S(X,X_1,K_y)$

$$S(X,X_1,K_y) = \left[\frac{\sin h\big(K_y(X_1 - X)\big)}{\sin h(K_yX_1)} - \frac{\sin h(X_1 - X)}{\sin h(X_1)}\right], \tag{4.9}$$

with the normalized coordinates $X \equiv k_{xn}x$, $X_1 \equiv k_{xn}L_\perp$, and $K_y \equiv k_y/k_{xn}$. This function is plotted versus X in Figures 2 for several values of X_1 and K_y. Although the SW eigenmodes for $E_{/\!/}^{(0)}$ are extinguished radially within one skin depth from

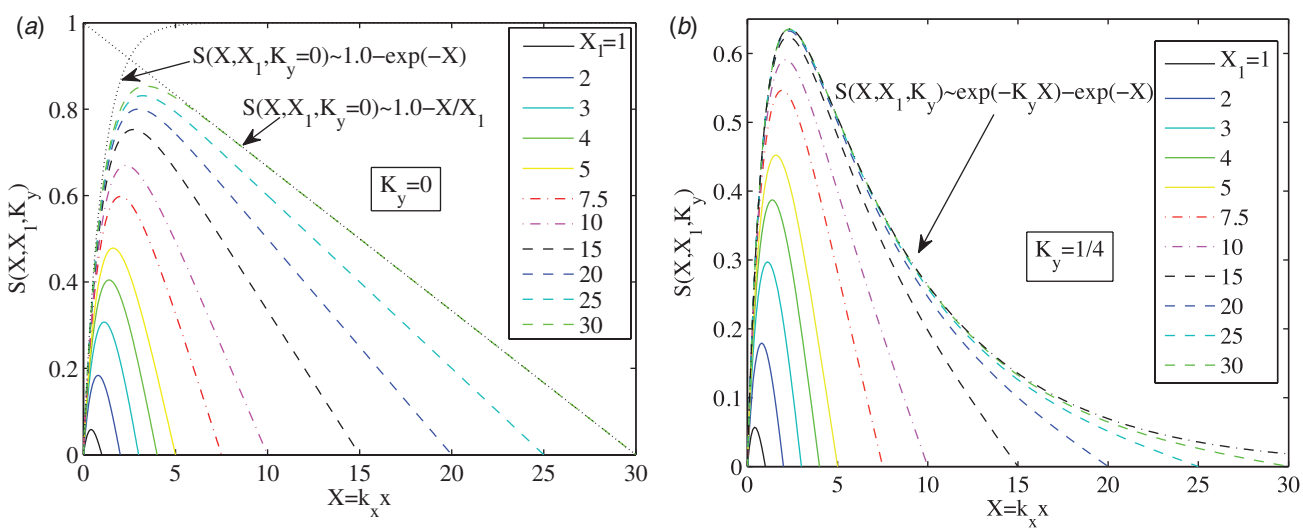

FIG. 2. Radial shape function $S(X, X_1, K_y)$ versus normalized coordinate $X = k_{xn}x$ for several values of $X_1 = k_{xn}L_\perp$ and (a) $K_y = 0$; (b) $K_y = 1/4$.

the SW cut-off layer, $V_{rf}^{(1)}$ can extend radially well beyond $X=1$. When $K_y X_1 \ll 1$ (Figure 2(a)), the sheath voltages are able to reach the inner boundary and a linear radial decay is found. Conversely for $K_y X_1 \gg 1$ (Figure 2(b)), exponential radial decay is found. The penetration depth of $V_{rf}^{(1)}$ can be estimated as $\min(L_\perp, 1/|k_y|)$. From Eq. (4.4), this radial behaviour can be interpreted as mode coupling of the leading order SW electric field $E_{//}^{(0)}$ to the first order SPW $V_{rf}^{(1)}$ *via* the RF sheaths.

B. Self-consistent first order RF + DC problem

$V_{rf}^{(1)}(x,y)$ being determined, the DC biasing problem can be solved at the first order in the asymptotic expansion to evaluate $V_{DC}^{(1)}(x,y,z)$. To proceed, we use again formula (2.14) in the limit $(\sigma_{//\mathrm{DC}}, \sigma_{\perp \mathrm{DC}}) \to (\infty, 0)$. We are mainly interested in the case $e|V_{rfl}|/kT_e \gg 1$, $e|V_{rfr}|/kT_e \gg 1$, when the DC plasma potential is far larger than kT_e/e. In this limit,

$$V_{DC}^{(1)}(x,y,z) \sim \max\left(|V_{rfl}^{(1)}(x,y)|, |V_{rfr}^{(1)}(x,y)|\right). \quad (4.10)$$

From this formula, the DC plasma potentials are expected to exhibit a similar radial extension as the RF sheath voltages. When the magnitude $E_{//ap}$ of the aperture RF field is increased, $V_{rf}^{(1)} \propto E_{//ap}$ and $V_{DC}^{(1)} \propto E_{//ap}$. The self-consistent 2D distribution $\delta(x,y)$ can be subsequently deduced from Eq. (2.15). It scales as $E_{//\mathrm{ap}}{}^{3/4}$. Finally, the first order corrections to the RF field can be evaluated, incorporating the nonlinearity due to the sheaths. $E_{//}^{(1)}(x,y,z)$ is governed by the SW equation (2.2) using Dirichlet BCs similar to Eq. (3.9), but with $E_{//}^{(1)}=0$ at the two radial boundaries. Consequently in a similar way as $E_{//}^{(0)}$ was decomposed into a discrete set of *toroidal* harmonic components, $E_{//}^{(1)}$ can be decomposed into *radial* harmonic components. The Fourier component $E_{//}^{(1)}(x,k_y,z)$ takes the form

$$E_{//}^{(1)}(x,k_y,z) = \sum_{m=1}^{\infty} C_m(k_y)\sin(k_{xm}x)\frac{\cosh(k_{//m}z)}{\cosh(k_{//m}L_{//m}/2)} + S_m(k_y)\sin(k_{xm}x)\frac{\sinh(k_{//m}z)}{\sinh(k_{//m}L_{//m}/2)}, \quad (4.11)$$

with $k_{xm}=m\pi/L_\perp$ and $k_{//m}^2 = -\varepsilon_\perp[k_0^2 - (k_{xm}^2+k_y^2)/\varepsilon_{//}] \approx -\varepsilon_\perp k_0^2$. From this expression, one can anticipate that $E_{//}^{(1)}$ will only be present within a toroidal distance of $1/k_0|\varepsilon_\perp|^{1/2}$ from the lateral boundaries. Another consequence of Eq. (4.11) is that the self-consistent total RF field $E_{//}^{(0)} + E_{//}^{(1)}$ cannot be split into eigenmodes. $E_{//}^{(1)}$ scales asymptotically as $V_{rf}^{(1)}/\delta \propto E_{//\mathrm{ap}}{}^{1/4}$, while $E_{//}^{(0)} \propto E_{//\mathrm{ap}}{}^{1}$. So the self-consistent asymptotic treatment becomes all the more accurate as the amplitude of the RF excitation (or equivalently the launched RF power) is increased.

C. Finite sheath width effects on the SPW

In order to discuss the validity of the asymptotic treatment, we would like here to assess how the finite δ affects the SPW. For this purpose, we follow Ref. 38: in this subsection δ is assumed known and homogeneous over the lateral boundaries. We then seek the SPW under the form of two plasma modes with symmetric and antisymmetric toroidal parity.

$$E_{//}(x,k_y,z) = E_{//even}\frac{\cosh(k_{//even}z)}{\cosh(k_{//even}L_{//}/2)}\frac{\sinh\left(k_{xeven}(L_\perp - x)\right)}{\sinh(k_{xeven}L_\perp)}. \quad (4.12)$$

The odd mode is similar, with $\sinh(k_{//odd}z)$ instead of $\cosh(k_{//even}z)$. The SPW verifies the full RF-SBC (2.6) on both sides of the simulation domain together with the SW equation (2.2). These constraints lead to a compatibility equation for $k_{//}$. For the even SPW mode[17]

$$\frac{\varepsilon_{//}\delta}{\varepsilon_{sh}}[k_0^2\varepsilon_\perp + k_{//even}^2] = -k_{//even}\tanh\left(\frac{k_{//even}L_{//}}{2}\right). \quad (4.13)$$

A similar equation holds for the odd mode with $\coth(\ldots)$ instead of $\tanh(\ldots)$. Equation (4.13) possesses a real solution for $k_{//}$. It is now solved to the leading order as $\delta \to \infty$.

$$k_{//even}{}^2 = k_{//odd}{}^2 = k_{//\infty}{}^2 = -k_0{}^2\varepsilon_\perp; k_{xeven} = k_{xodd} = k_y. \quad (4.14)$$

These asymptotic relations do not depend on δ. They correspond to the leading order RF-SBC (3.3) that was obtained without *a-priori* assumption about the sheath width spatial distribution. Substituting $k_{//}=(k_{//\infty}+dk_{//})$ into Eq. (4.13), the first order correction $dk_{//}$ to $k_{//\infty}$ is

$$dk_{//even} = -\frac{\varepsilon_{sh}}{2\varepsilon_{//}\delta}\tanh\left(\frac{k_{//\infty}L_{//}}{2}\right),$$
$$dk_{//odd} = -\frac{\varepsilon_{sh}}{2\varepsilon_{//}\delta}\coth\left(\frac{k_{//\infty}L_{//}}{2}\right). \quad (4.15)$$

And the associated corrections to the squared radial wavevector are

$$dk_{xeven}^2 = \frac{k_{//\infty}\varepsilon_{sh}}{\delta\varepsilon_\perp}\tanh\left(\frac{k_{//\infty}L_{//}}{2}\right),$$
$$dk_{xodd}^2 = \frac{k_{//\infty}\varepsilon_{sh}}{\delta\varepsilon_\perp}\coth\left(\frac{k_{//\infty}L_{//}}{2}\right). \quad (4.16)$$

For $\varepsilon_\perp < 0$, $|dk_{xodd}{}^2| > |dk_{xeven}{}^2|$. The first order corrections (4.16) to the SPW eigenmode (4.13) remain negligible at both lateral sides of the simulation domain as long as $|k_{xeven}-k_y|L_\perp \ll 1$, $|k_{xodd}-k_y|L_\perp \ll 1$. This requirement yields a simple criterion

$$\frac{\lambda_{crit}}{\delta} = \left|\frac{\varepsilon_{sh}}{\varepsilon_\perp^{1/2}}\frac{k_0 L_\perp^2}{\delta}\frac{1}{2\sqrt{\pi^2 + k_y^2 L_\perp^2}}\coth\left(\frac{k_{//\infty}L_{//}}{2}\right)\right| \ll 1. \quad (4.17)$$

In the self-consistent RF + DC approach, a typical value of the self-consistent inverse sheath widths $1/\delta$ should be used in the validity criterion, for example, their average over the simulation volume. Formula (4.17) provides a possible definition for the critical length λ_{crit} that will subsequently be tested numerically.

V. NUMERICAL TESTS OF ASYMPTOTIC RF THEORY

This part aims at assessing numerically the RF part of the SSWICH problem and its asymptotic treatment for wide sheaths. Tests were performed in a 2D (radial/parallel) rectangular domain similar to Figure 1, assuming constant values or harmonic oscillations as $\exp(ik_y y)$ in direction y (poloidal in a tokamak). A code solves the RF problem (2.2) with metallic boundary conditions at the inner radial boundary, prescribed RF field at the aperture, and the exact RF SBCs (2.6) at the lateral sides. Homogeneous plasma is assumed. The RF problem is discretized on a homogeneous 2D rectangular grid according to a finite difference scheme precise up to the second order in the spatial steps in both directions. Since we do not test the whole self-consistent RF + DC treatment, the sheath widths radial distributions $\delta_l(x)$ and $\delta_r(x)$ are prescribed throughout Sec. V but can vary with x. The numerical tests can be regarded as the effect on the RF wave of a coating on the lateral metallic walls with a specified spatially inhomogeneous thickness of dielectric material, in relation with realistic experiments.[18,48]

A. RF simulations with $E_{//} \neq 0$ at the sides of aperture

The reference RF simulation is performed with the following parameters representative of a high-density SOL near the ITER wall (magnetic field 3.93 T, electron density $5.25 \times 10^{18}\,\mathrm{m}^{-3}$, 50/50% D-T mix, RF frequency $f_0 = 47.5$ MHz):[49] $\varepsilon_{//} = -190\,000$; $\varepsilon_\perp = -63.4$; $\varepsilon_{sh} = 1.0$; $k_0 = 0.9955\ \mathrm{m}^{-1}$; $k_y = 0.0\,\mathrm{m}^{-1}$; $L_{//} = 3.0$ m; $L_\perp = 3$ cm. $\delta_l(x) = \delta_r(x) = \delta = 1$ mm constant with x. The system is excited with a flat unit RF field map

$$E_{//ap}(z) = 1\,V/m. \tag{5.1}$$

The RF excitation is non-zero at both sides of the aperture, so that the leading order asymptotic theory should apply. The parallel direction is divided into 257 space steps, while 301 steps are taken in the radial direction. This discretization resolves spatially all the characteristic parallel and radial scalelengths for both the SW and the SPW.

Figure 3(a) displays the 2D map for the simulated RF field $E_{//}$ accounting for the full RF-SBC. The antenna aperture is located in $x = 0$ at the bottom of the map. Two field structures are clearly visible. Far from the lateral boundaries of the system, the RF field map adopts the flat toroidal shape of the RF excitation, with a radial evanescence over the characteristic skin depth $\lambda_{skin} \sim c/\omega_{pe} \sim 2$ mm. This structure is expected from a SW field. On both sides of the domain, lateral wings develop, extending over the whole radial length of the simulation with amplitude similar to the excitation field. This structure is expected from a SPW due to the finite sheath width. It was checked that the wings completely disappear when the sheaths are suppressed. Figure 3(b) plots $E_{//}$ along several toroidal cross-sections through the simulated map. Far from the aperture, the RF field mainly exists near the lateral boundaries, with a toroidal extension of order $1/k_{//\infty} \sim 12.5$ cm characteristic of the SPW (see formula 4.14). The dashed line sketches the toroidal structure of the asymptotic even SPW eigenmode as $\cosh(k_{//\infty} z)$. $E_{//}$ decays toroidally along the dashed line and saturates near $z = 0$ at a level corresponding to the evanescent SW, i.e., this background level decreases radially as $\exp(-x/\lambda_{skin})$.

The specific role of the sheath width on the lateral wings indentified in Figure 3 is investigated in Figures 4 and 5. The lateral value of the RF electric field $E_{//}(x, z = -L_{//}/2)$ was plotted versus x over a series of simulations with the same parameters as the reference case, except the sheath width δ. When the profile $\delta(x)$ is flat, whatever its (large) value, the RF electric field decays linearly along the radial direction. Figure 4 also displays simulations with the sheath width $\delta(x)$ varying radially between half and twice the reference value, according to several profiles. Figure 4 shows that the RF field profile adjusts itself so that the product $\delta(x) E_{//}(x, z = -L_{//}/2)$ (and hence the RF voltage $V_{rf}(x)$) decays linearly along the lateral boundary, consistent with formula (3.5).

In Figure 5(a), the lateral electric field was plotted versus x over a scan of the homogeneous sheath width δ. The

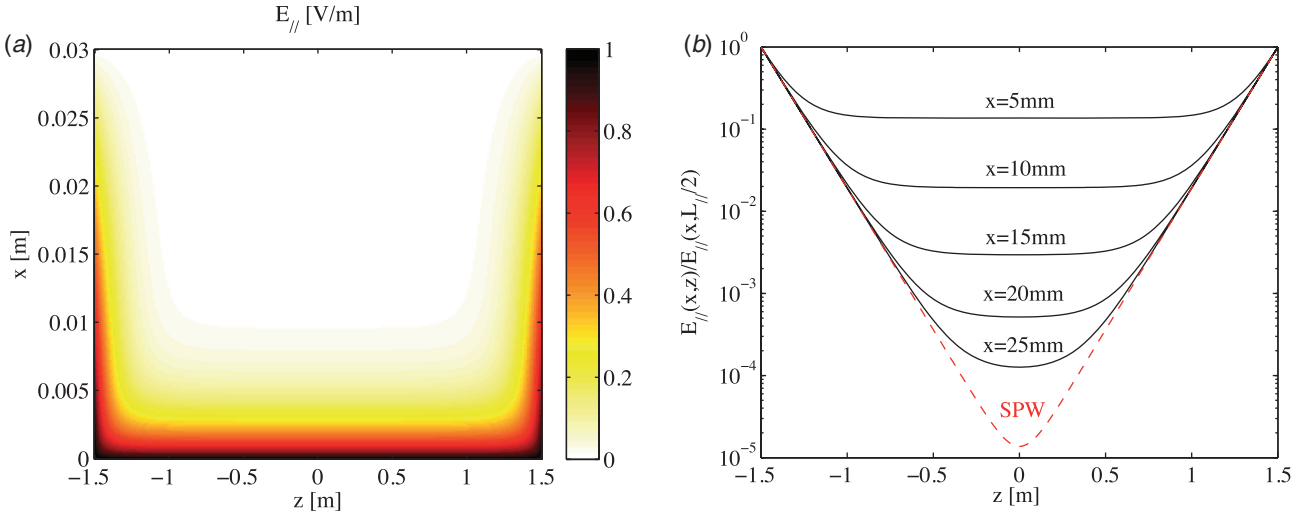

FIG. 3. RF field maps for the reference simulation. (a) 2D map (linear scale); (b) Selection of 1D radial cuts through the 2D map for several values of x. $E_{//}$ is normalized to its lateral value and is plotted in logarithmic scale.

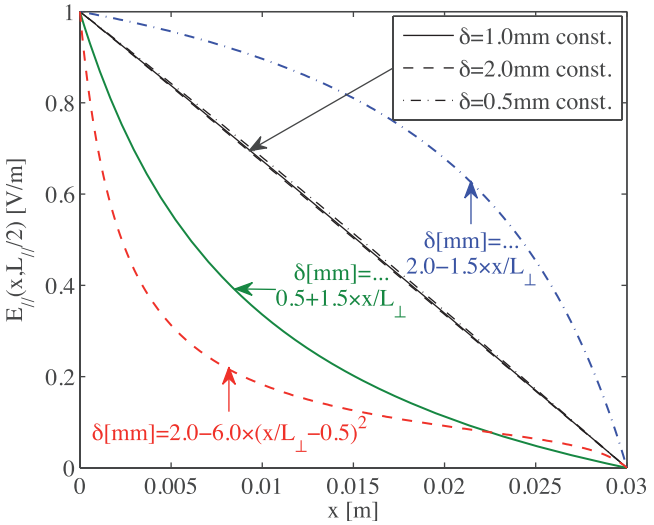

FIG. 4. Radial profile of the RF electric field at the left boundary of the simulation domain, for several values of the sheath width profile applied at both sides of the simulation.

radial profiles adopt a characteristic shape of the type $\sin(k_x(L_\perp - x))/\sin(k_x L_\perp)$. As δ increases, k_x tends to 0 and $E_{//}(x,L_{//}/2)$ progressively converges toward a linear profile. Multiplying the lateral electric field with $\varepsilon_{//}\delta/\varepsilon_{sh}$, one finds the RF voltage $V_{rf}(x)$. Figure 5(b) plots the relative difference $\Delta V_{rf}/V_{rf} = |1 - V_{rf}^{(0)}(x)/V_{rf}(x)|$ between the numerical value of $V_{rf}(x)$ and the asymptotic approximation $V_{rf}^{(0)}(x)$ from Eq. (3.5), showing more clearly the asymptotic convergence: $\Delta V_{rf}/V_{rf}$ roughly scales as $1/\delta$.

The parametric behaviour of $\Delta V_{rf}/V_{rf}$ was investigated more systematically in Figure 6. In a similar way as in Figure 5, the following parameters were scanned individually:

- Sheath width δ, with constant or parabolic radial distribution (see Figure 4)
- Radial extension $L_\perp$ of the simulation domain
- Poloidal wavevector k_y
- RF frequency (or equivalently k_0, keeping constant $\varepsilon_{//}$ and $\varepsilon_\perp$)
- Perpendicular dielectric constant $\varepsilon_\perp$ (keeping constant k_0 and $\varepsilon_{//}$).

The precision of the asymptotic treatment is quantified by the maximum of $\Delta V_{rf}/V_{rf}$ over the radial extension of the lateral walls. Figure 6 shows that the ratio λ_{crit}/δ defined by formula (4.17) using a radially averaged $1/\delta(x)$ is generally well representative of the deviation from the asymptotic theory. Some simulations were, however, outside this trend. Three main reasons were found:

- Either the asymptotic theory was predicted invalid ($\lambda_{crit}/\delta > 1$).
- Or the radial resolution Δx of the finite difference code was not sufficient to describe the radial evanescence of the SW and of the SPW ($k_y \Delta x > 1$).
- Or the toroidal resolution Δz of the finite difference code was not sufficient to describe the toroidal decay of the SPW ($k_0|\varepsilon_\perp|^{1/2}\Delta z > 1$).

B. RF simulations with $E_{//} = 0$ at the sides of aperture

A new reference RF simulation was performed with $E_{//} = 0$ at the sides of aperture. It shares the same parameters as the previous reference case, including the 2D discretization of the spatial domain. The system is now excited with the RF field map

$$E_{//ap}(z) = \sin\left(\pi(z/L_{//} + 1/2)\right). \tag{5.2}$$

The RF field is null at both sides of the aperture, so that $V_{rf}^{(0)} = 0$ and the first order asymptotic theory should apply. From Eq. (4.1), the excitation corresponds to the first asymptotic SW eigenmode of the waveguide, with unit amplitude.

Figure 7(a) displays the 2D map for the simulated $E_{//}$ and exhibits two structures. Far from the lateral boundaries of the system, the RF field map adopts the toroidal shape of the excitation RF field, with a radial evanescence over the characteristic skin depth $\lambda_{skin} \sim c/\omega_{pe} \sim 2$ mm. This structure is expected from the leading order SW field $E_{//}^{(0)}$ in the

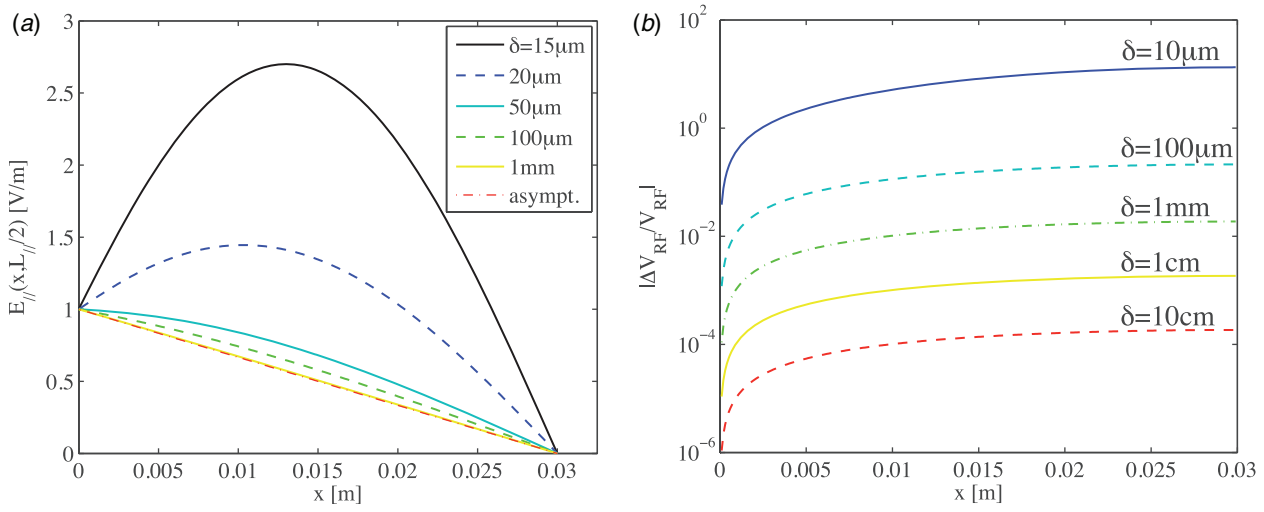

FIG. 5. (a) Lateral RF electric field versus x, for several sheath widths δ with flat profile. (b) Relative difference $\Delta V_{rf}/V_{rf} = |1 - V_{rf}^{(0)}(x)/V_{rf}(x)|$ of RF voltage $V_{rf}(x)$ with the asymptotic value $V_{rf}^{(0)}(x)$ from formula (3.5), versus x, for several values of δ.

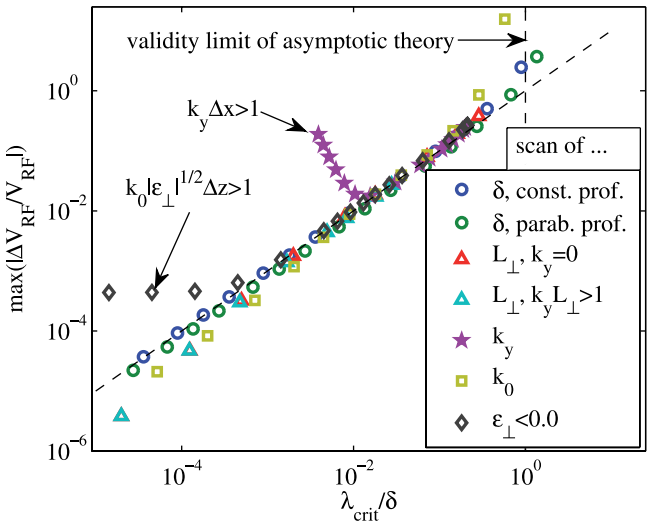

FIG. 6. Relative difference between the numerical RF voltages $V_{rf}(x)$ and leading order asymptotic value $V_{rf}^{(0)}(x)$ from formula (3.5), versus the ratio λ_{crit}/δ defined by formula (4.17). The maximum value of $\Delta V_{rf}/V_{rf} = |1 - V_{rf}^{(0)}(x)/V_{rf}(x)|$ over the radial extension of the simulation domain was retained.

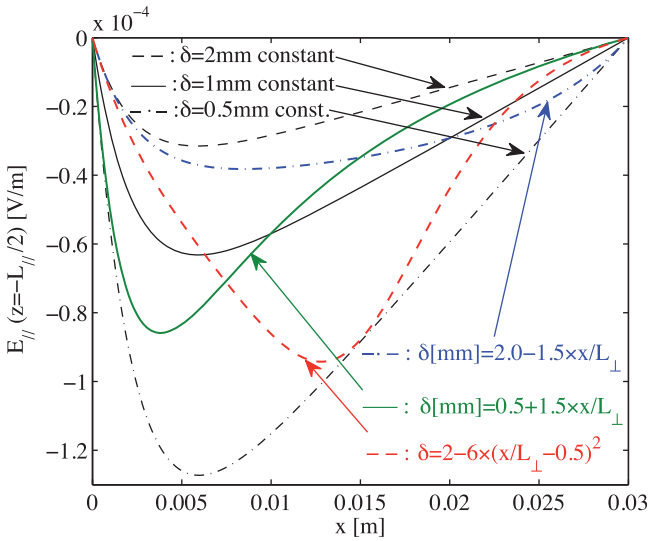

FIG. 8. Radial profile of the RF electric field at the left boundary of the simulation domain, for several values of the sheath width profile applied at both sides of the simulation.

asymptotic expansion. Although largely dominant, $E_{//}^{(0)}$ would produce no RF oscillations of the sheaths if taken alone, because its value at the lateral boundaries is strictly 0. On both sides of the domain small amplitude wings develop that are attributed to the first order corrections $E_{//}^{(1)}$. In Figure 7(b), the leading order RF field $E_{//}^{(0)}$ from formula (4.1) was subtracted from the simulated $E_{//}$, showing more clearly the corrections. They mainly exist near the lateral boundaries, with a toroidal extension of order $1/k_{//\infty} \sim 12.5$ cm. They extend radially up to the inner boundary. These two properties are characteristic of the asymptotic SPW. Corrections have a typical amplitude 10^{-4} lower than the RF excitation. But their non-zero value at the lateral boundaries is essential to excite RF sheaths. The large ratio of amplitudes between the successive approximations to the RF field is the main motivation for our asymptotic approach.

In Figure 8, the lateral electric field $E_{//}(x, z = -L_{//}/2)$ was plotted versus x over a series of simulations with the same parameters as the reference case, except the sheath width $\delta(x)$. When δ is doubled, the computed field is roughly halved, with the same radial profile. Figure 8 also displays simulations with the sheath width $\delta(x)$ varying radially between half and twice the reference value, according to several profiles. Figure 8 shows that as $\delta(x)$ changes the profile $E_{//}(x, z = -L_{//}/2)$ adjusts itself so that the product $\delta(x)E_{//}(x, z = -L_{//}/2)$ (and hence the RF voltage $V_{rf}(x)$) keeps the same value as in the reference simulation. This behaviour is consistent with the first order asymptotic formula (4.8) and is essential in view of self-consistent computations with more realistic input RF field maps: the asymptotic $V_{rf}(x)$ can be calculated without knowing *a priori* the self-consistent spatial distribution $\delta(x)$.

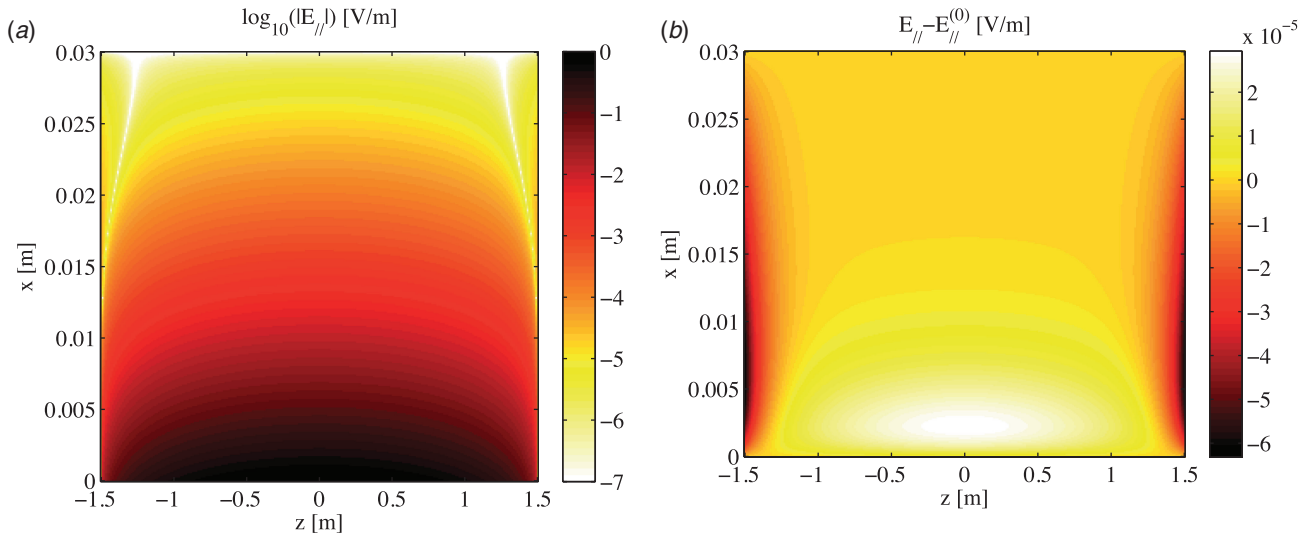

FIG. 7. 2D RF field maps for the new reference simulation. (a) Absolute value of total RF field (log scale); (b) correction to leading order RF field (linear scale).

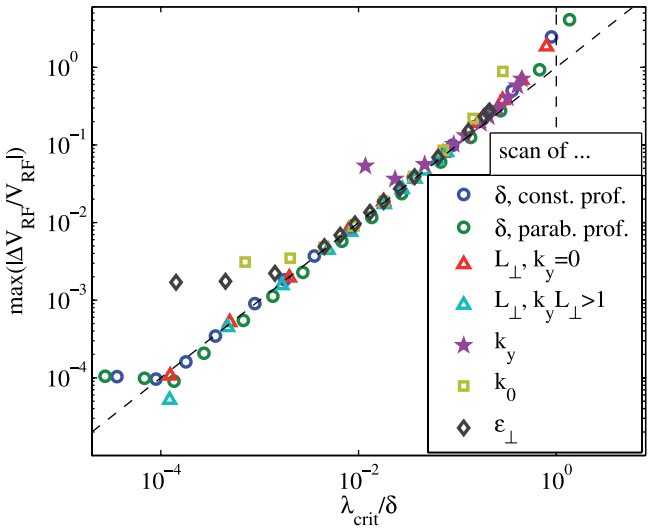

FIG. 9. Relative difference of the numerical RF voltages $V_{rf}(x)$ with first order asymptotic value $V_{rf}^{(1)}(x)$ from formula (4.8) versus the ratio λ_{crit}/δ defined by formula (4.17). The maximum value of $\Delta V_{rf}/V_{rf} = |1 - V_{rf}^{(1)}(x)/V_{rf}(x)|$ over x was retained.

The deviation of the RF voltages $V_{rf}(x)$ from their first order approximation $V_{rf}^{(1)}(x)$ from formula (4.8) was investigated systematically in Figure 9. λ_{crit}/δ from formula (4.17) is generally a good indicator for the deviation from the asymptotic theory. Some simulations were however outside this trend, for the same numerical reasons as previously. To correctly estimate the sheath voltages, a precise estimate of $E_{//}^{(1)}$ is necessary. But since over most of the simulation domain $|E_{//}^{(1)}| \ll |E_{//}^{(0)}|$, any numerical approach that does not separate the successive asymptotic contributions needs to be extremely accurate to produce reliable results (all the more accurate as λ_{crit}/δ gets large). The practical consequence is a poor convergence of the full RF + DC simulations for high RF power injected. On the contrary, the asymptotic approach gets more precise as the self-consistent δ get large, and therefore usefully complements more "usual" methods for high RF power simulations.

VI. CONCLUSIONS AND PROSPECTS

Motivated by a closer proximity to the first principles and the allowance for DC current circulation in the SOL plasma of magnetic fusion devices, this paper described the ICRF wave propagation self-consistently with the DC biasing of open magnetic field lines within a minimal fluid approach. The RF and DC parts were coupled by non-linear SBCs at both ends of open field lines. Only a simplified framework was described, featuring slow wave (SW) only and walls normal to $\mathbf{B_0}$.

In order to gain insight into the non-linear physics of the full DC + RF model and to provide a first guess for the iterative resolution algorithms, the self-consistent system was solved explicitly in the asymptotic limit when the sheath widths get very large, for any 2D input RF field excitation, in presence of a radial profile for the plasma parameters. Within a perturbative development of the RF SBCs up to lowest relevant order depending on the input field map, the propagation of oscillating sheath voltages $V_{rf}(x,y)$ along the lateral walls amounts to a linear problem that can be solved without prior knowledge of the self-consistent radial/poloidal distribution of the sheath widths $\delta(x,y)$. Consistent with this result, it was found numerically that for given $\delta(x)$, the lateral RF field profile $E_{//}(x)$ adjusts itself so that the product $\delta(x)E_{//}(x)$ converges asymptotically to a known function of x. In the first order case, the RF voltages were deduced from the parallel derivative of the leading order RF electric field, through its convolution with a simple Green's function. In parallelepipedic geometry, semi-analytical results were proposed in terms of asymptotic SW eigenmodes that could easily be implemented numerically without restriction on $\delta(x,y)$.

Throughout the resolution, basic physical properties of the asymptotic solution were outlined. It was shown that the RF voltages could propagate radially along the lateral boundaries much further away than the skin depth c/ω_{pe} characteristic of the SW evanescence. This has potentially important impact for RF plant operation, for the design of future antennae and interaction with high-Z metallic plasma facing components. This conclusion is qualitatively similar to Ref. 38. But the details of the radial distributions differ in the two papers, due to the different assumptions made. We believe that if radiation conditions are applied in the present model while sheath widths get large in Ref. 38, the radial profiles of $V_{rf}(x)$ in the two papers converge to a common solution. Since $V_{rf}(x) \propto E_{//}(x)\delta(x)$ and $\delta(x)$ is different in the two models, then the field maps $E_{//}(x)$ will differ at the lateral boundaries. Well beyond the skin depth, several regimes of radial propagation were identified depending on $k_y L_\perp$, the product of the poloidal wave-vector by the radial extension of the bounded SOL. Associated with the RF voltages, RF electric fields developed along the lateral walls of the SOL plasma, with a toroidal extension of the order of $1/(k_0|\varepsilon_\perp|^{1/2})$ away from the lateral boundaries. These characteristics were illustrated by RF simulations and were ascribed to the dispersion properties of the SPW, a new wave branch introduced by the RF-SBCs. In the "wide sheaths" limit, the RF voltage development amounts to the excitation and propagation of the SPW, either directly at the antenna aperture (leading order) or *via* mode coupling from the SW (first order). For easier iterations, V_{rf} was therefore treated as independent of $E_{//}$ in a 3-field re-formulation of the RF + DC problem.

The SPW radial penetration led to re-discuss the choice of the boundary conditions at the inner plasma side of the simulation volume. It was proposed to choose the radial extension $L_\perp$ as the radial penetration depth of the material objects surrounding the RF antenna, since the SPW cannot propagate in the absence of lateral material boundaries. More clever choices can be envisaged in more complex geometries featuring protruding objects in a parallelepipedic box.[27] The scalar wave equation (2.2) was also questioned, since it applies only to short-wavelength modes with the ordering $|k_\perp^2| \gg k_0^2|\varepsilon_\perp|$.[34,36] Equation (2.2) can only be assessed within a broader approach incorporating all the RF field polarizations. Therefore, this was left for further study.

In the self-consistent RF + DC model, the asymptotic scaling of various physical quantities with the amplitude $E_{//ap}$ of the input RF excitation (or equivalently with the launched RF power $P_{RF} \propto E_{//ap}^2$) was also studied,

depending on the lowest relevant order in the asymptotic expansion. This parametric dependence is valuable for design and experimental studies. In particular, the RF-induced heat loads in the RF antenna vicinity were inferred experimentally to scale as $E_{//ap}$[1,29,30] consistent with the first order theory. The particular simulation showed in Ref. 38 also scales asymptotically as our first order theory. The scaling suggests that the asymptotic approach should apply above some value of the launched RF power. To discuss more deeply this validity, a quantitative indicator was exhibited as a function of the main model parameters and tested against 2D RF simulations with prescribed radial profiles of the sheath width.

Within its domain of validity, the asymptotic solution can be applied for RF sheath assessment using at the aperture realistic 2D (toroidal/poloidal) maps of the parallel RF field from antenna codes.[3,4] Alternatively, the RF + DC system could be excited *via* current straps inside the simulation domain, while metallic conditions or SBCs are enforced at the outer wall. This case is similar to the first order theory. The principle of a subsequent iterative refinement of the solution from the asymptotic results was sketched. It remains however to be experimented, with, e.g., the goal of "selecting" a specific solution out of potential multiple roots for the nonlinear coupled RF + DC problem.[26,38] The convergence of this iterative scheme remains an open issue. Although it was presented in a simplified parallelepipedic geometry, the asymptotic method can be implemented numerically in its present form on more complex 3D simulation domains as long as lateral boundaries are kept normal to $\mathbf{B_0}$. This implementation has started, with the goal of simulating sheaths on Tore Supra antenna side limiters and understanding the experimental behaviour of a new type of Faraday screen.[27]

The asymptotic principle presented here is general and could *a priori* be generalized to more complex cases through a perturbative treatment of the more general RF-SBC (2.3). Within the SSWICH project, a more realistic self-consistent description of the RF physics in the plasma edge could therefore be envisaged, by progressively incorporating full RF field polarization, shaped wall, excitation by straps, perfectly matched layers at the inner boundary,[50] more realistic models of DC plasma conductivity, or RF-induced density modification.

ACKNOWLEDGMENTS

This work, supported by the European Communities under the contract of Association between EURATOM and CEA, was carried out within the framework of the European Fusion Development Agreement. The views and opinions expressed herein do not necessarily reflect those of European Commission.

[1]J.-M. Noterdaeme and G. Van Oost, Plasma Phys. Controlled Fusion **35**, 1481 (1993) and references therein.
[2]F. W. Perkins, Nucl. Fusion **29**(4), 583 (1989).
[3]S. Pécoul, S. Heuraux, R. Koch, and G. Leclert, Comput. Phys. Commun. **146**, 166–187 (2002).
[4]V. Lancellotti, D. Milanesio, R. Maggiora, G. Vecchi, and V. Kyrytsya, Nucl. Fusion **46**, S476–S499 (2006).
[5]J. Myra, D. D'Ippolito, and Y. Ho, Fusion Eng. Des. **31**, 291 (1996).
[6]D. A. D'ippolito, J. R. Myra, J. H. Rogers, K. W. Hill, J. C. Hosea, R. Majeski, G. Schilling, J. R. Wilson, G. R. Hanson, A. C. England, and J. B. Wilgen, "Analysis of RF sheath interactions in TFTR," Nucl. Fusion **38**(10), 1543–1563 (1998).
[7]L. Colas, S. Heuraux, S. Brémond, and G. Bosia, Nucl. Fusion **45**, 767–782 (2005).
[8]V. Bobkov, R. Bilato, F. Braun, L. Colas, R. Dux, D. Van Eester, L. Giannone, M. Goniche, A. Herrmann, P. Jacquet, A. Kallenbach, A. Kryvska, E. Lerche, M.-L. Mayoral, D. Milanesio, I. Monakhov, H.-W. Müller, R. Neu, J.-M. Noterdaeme, Th. Pütterich, V. Rohde, ASDEX Upgrade Team, and JET-EFDA Contributors, AIP Conf. Proc. **1187**, 125–132 (2009).
[9]A. Krivska, D. Milanesio, V. Bobkov, F. Braun, J. M. Noterdaeme, and ASDEX Upgrade team, "Electromagnetic simulations of the ASDEX Upgrade ICRF antenna with the TOPICA code," AIP Conf. Proc. **1187**, 137–140 (2009).
[10]Vl. V. Bobkov, F. Braun, R. Dux, A. Herrmann, L. Giannone, A. Kallenbach, A. Krivska, H.-W. Müller, R. Neu, J.-M. Noterdaeme, T. Pütterich, V. Rohde, J. Schweinzer, A. Sips, I. Zammuto, and ASDEX Upgrade Team, Nucl. Fusion **50**, 035004 (2010).
[11]A. Mendes, L. Colas, K. Vulliez, A. Ekedahl, A. Argouarch, and D. Milanesio, "Reduction of RF-sheaths potentials by compensation or suppression of parallel RF currents on ICRF antennas," Nucl. Fusion **50**, 025021 (2010).
[12]M. Sorba, D. Milanesio, R. Maggiora, and A. Tuccillo, Fusion Eng. Des. **85**(2), 161–168 (2010).
[13]D. Milanesio and R. Maggiora, Nucl. Fusion **50**, 025007 (2010).
[14]R. Maggiora and D. Milanesio, "Mitigation of parallel RF potentials by an appropriate antenna design using TOPICA," AIP Conf. Proc. **1406**, 73–80 (2011).
[15]M. L. Garrett and S. J. Wukitch, "Mitigation of radio frequency sheaths through magnetic field-aligned ICRF antenna design," Fusion Eng. Des. (submitted).
[16]L. Colas, A. Ekedahl, M. Goniche, J.-P. Gunn, B. Nold, Y. Corre, V. Bobkov, R. Dux, F. Braun, J.-M. Noterdaeme, M.-L. Mayoral, K. Kirov, J. Mailloux, S. Heuraux, E. Faudot, J. Ongena, ASDEX Upgrade Team, and JET-EFDA Contributors, Plasma Phys. Controlled Fusion **49**, B35–B45 (2007).
[17]D. A. D'Ippolito and J. R. Myra, Phys. Plasmas **13**, 102508 (2006).
[18]S. J. Wukitch, B. LaBombard, Y. Lin, B. Lipschultz, E. Marmar, M. L. Reinke, D. G. Whyte, and Alcator C-Mod Team, "ICRF specific impurity sources and plasma sheaths in Alcator C-Mod," J. Nucl. Mater. **390–391**, 951–954 (2009).
[19]E. Faudot, S. Heuraux, L. Colas, and J. P. Gunn, "Broadening of rectified potential structures induced by RF currents in a magnetized plasma: Application to ITER scrape-off-layer," Phys. Plasmas **17**, 042503 (2010).
[20]R. Van Nieuwenhove and G. Van Oost, Plasma Phys. Controlled Fusion **34**, 525 (1992).
[21]J. P. Gunn, L. Colas, A. Ekedahl, E. Faudot, V. Fuchs, S. Heuraux, M. Goniche, M. Kočan, A. Mendes, A. Ngadjeu, V. Petržilka, F. Saint-Laurent, and K. Vulliez, in *Proceedings of the 22nd IAEA Fusion Energy Conference Geneva* (2008), EX/P6-32.
[22]M. A. Lieberman, IEEE Trans. Plasma Sci. **16**, 638 (1988).
[23]V. Godyak and N. Sternberg, Phys. Rev. A **42**, 2299 (1990).
[24]E.-F. Jaeger, L.-A. Berry, J.-S. Tolliver, and D.-B. Batchelor, "Power deposition in high-density inductively coupled plasma tools for semiconductor processing," Phys. Plasmas **2**(6), 2597–2604 (1995).
[25]B. Van Compernolle, R. Maggiora, G. Vecchi, D. Milanesio, and R. Koch, "Implementation of sheath effects into TOPICA," in *Proceedings of the 35th EPS Conference on Plasma Physics* (2008), ECA Vol. 32, P2.105.
[26]H. Kohno, J. R. Myra, and D. A. D'Ippolito, Phys. Plasmas **19**, 012508 (2012).
[27]J. Jacquot, D. Milanesio *et al.*, "Recent advances in self-consistent RF sheath modelling and related physical properties: Application to Tore Supra IC antennae," in *Proceedings of the 39th EPS Conference on Plasma Physics and Controlled Fusion, Stockholm* (2012), ECA Vol. 36F, P2.038, http://ocs.ciemat.es/EPSICPP2012PAP/pdf/P2.038.pdf.
[28]B. Lipschultz, D. A. Pappas, B. LaBombard, J. E. Rice, D. Smith, and S. J. Wukitch, Nucl. Fusion **41**, 585 (2001).
[29]L. Colas, V. Basiuk, B. Beaumont, A. Bécoulet, G. Bosia, S. Brémond, M. Chantant, F. Clairet, A. Ekedahl, E. Faudot, A. Géraud, M. Goniche, S. Heuraux, G.-T. Hoang, G. Lombard, L. Millon, R. Mitteau, P. Mollard, K. Vulliez, and Tore Supra Team, Nucl. Fusion **46**(7), S500–S513 (2006).

[30]P. Jacquet, L. Colas, M.-L. Mayoral, G. Arnoux, V. Bobkov, M. Brix, P. Coad, A. Czarnecka, D. Dodt, F. Durodié, A. Ekedahl, D. Frigione, M. Fursdon, E. Gauthier, M. Goniche, M. Graham, E. Joffrin, A. Korotkov, E. Lerche, J. Mailloux, I. Monakhov, C. Noble, J. Ongena, V. Petrzilka, C. Portafaix, F. Rimini, A. Sirinelli, V. Riccardo, Z. Vizvary, A. Widdowson, K.-D. Zastrow, and JET EFDA Contributors, "Heat-loads on JET plasma facing components from ICRF and LH wave absorption in the SOL," Nucl. Fusion **51**, 103018 (2011).
[31]D. A. D'Ippolito, J. R. Myra, J. Jacquinot, and M. Bures, Phys. Fluids B **5**(10), 3603 (1993).
[32]G.-R. Hanson, A.-C. England, J.-B. Wilgen, F.-W. Baity, D.-B. Batchelor, M.-D. Carter, D.-J. Hoffman, M. Murakami, D. A. Rasmussen, P.-M. Ryan, D. W. Swain, J.-H. Rogers, J.-R. Wilson, R.-P. Majeski, G. Schilling, E.-J. Doyle, and K.-W. Kim, in *Proceedings of the 11th Topical RF Conference, Palm Springs, CA, USA, May* (1995), p. 463.
[33]C. Lau, G. Hanson, Y. Lin, O. Meneghini, S. Wukitch, B. Labombard, R. Parker, S. Shiraiwa, G. Wallace, J. Wilgen, and ALCATOR C-miod Team, "Effect of ICRF and LHCD on SOL density profiles on ALCATOR C-mod," AIP Conf. Proc. **1406**, 227–230 (2011).
[34]T. H. Stix, *The Theory of Plasma Waves* (McGraw Hill, 1962).
[35]M. D. Carter, P. M. Ryan, D. Hoffman, W. S. Lee, D. Buschberger, and V. Godyak, "Combined rf and transport effects in magnetized capacitive discharges," J. Appl. Phys. **100**, 073305 (2006).
[36]D. A. D'Ippolito and J. R. Myra, Phys. Plasmas **16**, 022506 (2009).
[37]D. A. D'Ippolito and J. R. Myra, Phys. Plasmas **17**, 072508 (2010).
[38]J. R. Myra and D. A. D'Ippolito, Plasma Phys. Controlled Fusion **52**, 015003 (2010).
[39]A. Rozhansky, Rev. Plasma Phys. **24**, 1–52 (2008).
[40]Ph. Ghendrih, Y. Sarazin, G. Attuel, S. Benkadda, P. Beyer, G. Falchetto, C. Figarella, X. Garbet, V. Grandgirard, and M. Ottaviani, "Theoretical analysis of the influence of external biasing on long range turbulent transport in the scrape-off layer," Nucl. Fusion **43**, 1013–1022 (2003).
[41]D. A. D'Ippolito, J. R. Myra, P. M. Ryan, E. Righi, J. Heikkinen, P. U. Lamalle, J.-M. Noterdaeme, and Contributors to the EFDA–JET Workprogramme, Nucl. Fusion **42**, 1357–1365 (2002).
[42]A. Ngadjeu, E. Faudot, L. Colas, S. Heuraux, J. Gunn, and M. Kubič, "Generation of DC currents by ICRF near fields in the scrape-off layer," J. Nucl. Mater. **415**, S1009–S1012 (2011).
[43]R. Chodura, Phys. Fluids **25**(9), 1628 (1982).
[44]C. D. Child, Phys. Rev. (Series I) **32**, 492 (1911).
[45]I. Langmuir, Phys. Rev. **2**, 450 (1913).
[46]I. Langmuir and K. Blodgett, Phys. Rev. **22**, 347 (1923).
[47]J. R. Myra, D. A. D'Ippolito, J. A. Rice, and C. S. Hazelton, J. Nucl. Mater. **249**, 190–198 (1997).
[48]J. Sorensen, D.-A. Diebold, R. Majeski, and N. Hershkowitz, "Edge power deposition reduction in a tokamak by replacing the Faraday screen on an RF antenna with an insulator," Nucl. Fusion **36**(2), 173–190 (1996).
[49]S. Carpentier and R. A. Pitts, "Estimated density and temperature profiles in front of the IC ITER antenna during burning flat-top (inductive scenario 1, 15 MA, $Q_{DT} = 10$)," ITER_D_33Y59M-v2.3, 2010.
[50]J. Jacquot, "Perfectly matched layers for radiofrequency wave propagation in gyrotropic media," private communication (2011).